MiR-223-3p Regulates Autophagy and Inflammation by Targeting ATG16L1 in *Fusarium solani*–Induced Keratitis

Hanfeng Tang, Yi Lin, Liwei Huang, and Jianzhang Hu

Department of Ophthalmology, Fujian Medical University Union Hospital, Fu Zhou, China

Correspondence: Jianzhang Hu, Department of Ophthalmology, Fujian Medical University Union Hospital, 29 Xinquan Road, Fuzhou 350005, China; ophhjz@163.com.

HT and YL contributed equally to this article.

Received: October 3, 2021
Accepted: January 5, 2022
Published: January 28, 2022

Citation: Tang H, Lin Y, Huang L, Hu J. MiR-223-3p regulates autophagy and inflammation by targeting ATG16L1 in *Fusarium solani*–induced keratitis. *Invest Ophthalmol Vis Sci.* 2022;63(1):41. https://doi.org/10.1167/iovs.63.1.41

Purpose. Increasing evidence suggested that microRNAs (miRs) are implicated in the regulation of the inflammatory response and autophagy in multiple diseases. The present study aimed to explore the effect of miR-223-3p on inflammation and autophagy in fungal keratitis (FK).

Methods. An FK mouse model was established, and primary corneal stromal cells were isolated by inoculation with *Fusarium solani*. The expression of miR-223-3p was determined by quantitative RT-PCR. Subsequently, the target gene of miR-223-3p was identified by a dual-luciferase reporter assay. The levels of miR-223-3p were altered by transfecting miR agomir/antagomir to evaluate its effects. Slit-lamp biomicroscopy and hematoxylin and eosin staining were employed to detect corneal damage. The levels of autophagy were assessed by immunofluorescence, Western blotting, mRFP-GFP-LC3 fluorescence microscopy, and electron microscopy. In addition, inflammation was demonstrated by determining the proinflammatory mediators IL-1β and TNF-α.

Results. Our data suggested that miR-223-3p was increased and that autophagic flux was impaired in mouse FK. Then, we confirmed that autophagy-related gene 16L1 (ATG16L1) was a potential target of miR-223-3p and that this miR negatively regulated the expression of ATG16L1. The inhibition of miR-223-3p attenuated inflammation in FK, reduced P62 expression, and increased the ratio of LC3-II/LC3-I, whereas the overexpression of miR-223-3p displayed the opposite results.

Conclusions. Taken together, miR-223-3p might regulate autophagy via targeting ATG16L1 in experimental *F. solani* keratitis and is associated with the inflammatory response. MiR-223-3p might be a potential therapeutic target for FK.

Keywords: fungal keratitis, *Fusarium solani*, autophagy, miR-223-3p, ATG16L1

Fungal keratitis (FK) is an infectious disease of the cornea that leads to severe visual impairment.[1] According to previous studies, FK has shown a prominently increasing morbidity, accounting for 20% to 60% of infectious keratitis in tropical and subtropical regions.[2] Among them, *Fusarium solani* is the most common species that causes FK in many countries.[3] The cornea is the frontline defender against invading pathogenic fungi by providing a mechanical barrier and initiating an immune and inflammatory response.[4] Excessive immune reactions and inflammatory responses play a crucial role in the injured cornea.[5] However, its pathogenesis is not fully understood, which limits its effective therapy.[6,7] Thus, it is urgent to unravel the pathogenesis of FK and develop effective treatment strategies.

MicroRNAs (miRs) are highly conserved endogenous noncoding single-stranded small RNA molecules that regulate the expression of the protein-coding gene after transcription by binding with the 3′ untranslated region (3′UTR) of mRNAs.[8,9] Increasing evidence has illustrated that miRs are involved in the regulation of inflammatory response in multiple diseases.[10–12] Recent studies revealed that miR-223-3p is an essential regulator of inflammation and infection.[13,14] MiR-223-3p could regulate signal transducer and transcription activator 3 expression in macrophages triggered by Toll-like receptors, which are bound up with inflammatory responses in macrophages during microbial infection.[15] Long et al.[16] further demonstrated that miR-223-3p targeting the NOD-like receptor protein 3 could suppress inflammasome activation in endothelial cells infected with *Treponema pallidum* subsp. *pallidum*. Of note, previous studies found that the levels of miR-223-3p were obviously increased in *F. solani*–infected mouse corneal tissues.[17,18] Nonetheless, the potential mechanism and biological role of miR-223-3p in FK have not been well revealed.

Autophagy is a highly conservative catabolism process in eukaryotes that is very important to maintain in intracellular homeostasis, whereas autophagy dysfunction leads to the occurrence of diseases.[19,20] A previous study indicated that autophagy was altered in the mouse corneas after infection with *Aspergillus fumigatus* and played an anti-inflammatory role in the innate immune response.[21] Our previous findings also suggested that autophagy plays an indispensable role during the occurrence of FK.[17] However, the upstream pathway of autophagy in FK is unclear; thus, we attempted to identify key upstream regulators

of autophagy. More recently, the regulatory influence of miR-223-3p on autophagy has attracted increasing attention.[22,23] For instance, the inhibition of miR-223-3p suppresses autophagy and reduces cisplatin resistance in non–small cell lung carcinoma via targeting F-box/WD repeat-containing protein 7 (FBXW7).[24] Hu et al.[22] pointed out that the knockdown of miR-223-3p activates the pathway of autophagy by enhancing forkhead box O3 (FOXO3) in an atrial fibrillation model. Hence, we are curious about whether miR-223-33p, which is notably increased in fungal keratitis, can also regulate autophagy.

To explore the role of miR-223-3p in autophagy in FK, changes in autophagy and the inflammatory response were detected through modulating miR-223-3p expression. Our research aimed to identify miR-223-3p as a prognostic biomarker and potential therapeutic target for the treatment of FK.

Materials and Methods

Fungal Species

The standard fungal strain *F. solani* (AS 3.1829) used in the study was obtained from the China General Microbiological Culture Collection Center (CGMCC, Beijing, China), originally isolated from human skin. The fungal strain was inoculated on Sabouroud medium (lot. 1900518; OXOID, Basingstoke, Hampshire, UK) by the scratch method and cultured at 28°C for 7 days.

Preparation of Fungal Suspensions

Sterile PBS (1 mL) was added to the petri dish; the mycelia and conidia were scraped, and the mixed solution was collected. Then, the mycelia were removed by filtration with sterile gauze. After that, the conidia were adjusted with sterile water to a concentration of 1×10^8 CFU/mL. Finally, the conidial suspension could be used for subsequent experiments.

Experimental Animals

BALB/C (6–8 weeks) mice were obtained from Charles River Lab Biological Technology Co., Ltd (Beijing, China). We performed a slit-lamp examination to ensure that the eyeballs of mice were healthy. During the rearing and testing of mice, we strictly followed the guidance from ARVO. Before being infected by *F. solani*, mice were randomized into the following four groups ($n = 6$/group): miR-NC (RiboBio Co. Guangzhou, China; miR3N0000001-4-5), miR-223 (miR41236163457), Ant-223 (miR30000665), and the control group. The FK models were implemented based on a previous protocol.[25] Briefly, mice were injected intraperitoneally with a pentobarbital suspension (50 mg/kg). Subsequently, the corneal epithelium (approximately 2.5 mm in diameter) was removed with an electric scraper. Then, the full-thickness rat cornea was cut along the corneal limbus under relatively sterile conditions and made into soft contact lenses with a diameter of about 5 mm to cover the mouse corneas. After the mouse eyelids were sutured with 5-0 silk thread, 5 µL fungal suspension was injected into the conjunctival sac. Next, the contact lenses were removed after incubation for 24 hours, while the mouse eyelid sutures were dismantled. The corneas of mice were carefully observed and photographed daily under a slit-lamp microscope. According to the previously described scoring system,[26] a clinical score from 0 to 12 was used to assess the severity of FK. A grade from 0 to 4 was assigned to each item: opacity density, opacity area, and surface regularity. The total scores from these three categories were classified as mild (score 0–5), moderate (score 6–9), or severe (score 10–12). Corneas were harvested for the following experiments.

Hematoxylin and Eosin Staining

The corneas of mice from different groups were harvested and immersed with 4% paraformaldehyde (Sigma-Aldrich, St. Louis, MO, USA) overnight. After being dehydrated in gradient alcohol, the samples were embedded with paraffin and sectioned with an ultramicrotome. Paraffin sections were dewaxed with xylene, rehydrated with gradient alcohol, and rinsed three times. The tissues were immerged in hematoxylin solution for 5 minutes, followed in eosin solution for 1 to 2 minutes; dehydrated with gradient alcohol; and finally mounted with neutral resin. After hematoxylin and eosin (HE) staining, tissues were observed with an optical microscope (Nikon, Tokyo, Japan).

Primary Cell Culture

The removed mouse eyeballs were washed with sterile PBS containing penicillin and streptomycin (100 U/mL, TMS-AB2-C; Merck Millipore, Boston, MA, USA) three times. Each eyeball was digested for 12 hours at 4°C with 150 µL dispaseII enzyme (15 mg/mL; Sigma-Aldrich). Next, the corneal tissues were cut into small fragments after the removal of loose corneal epithelium. Furthermore, the tissues were digested with collagenase A (10 mg/mL; Sigma-Aldrich) at 37°C for 1 hour. Then, corneal stromal cells were suspended in a 25-cm^2 culture flask with DF12 medium (DMEM F-12; Sigma-Aldrich). Adherent cells were observed after 10 to 12 hours at 37°C.

Cell Transfection

The corneal stromal cells (1×10^5 cells/well) were divided randomly into four groups: miR-223-3p NC (miR-NC) group, miR-223-3p agomir (miR-223) group, miR-223-3p antagomir (Ant-223) group, and control group (without any treatment). Then, according to standard protocols, we transfected them (at a density of 60%–70%) with the respective miR reagent at 100 nM using Lipofectamine 2000 (Thermo Fisher Scientific; Invitrogen, Inc., Massachusetts, USA). Fresh medium containing penicillin and streptomycin was replaced after 8 hours, and the incubation was continued for 48 hours.

RNA Extraction

The mouse corneas or corneal stromal cells were harvested. Each mouse cornea was digested with 800 µL TRIzol reagent (Takara Bio, Inc., Tokyo, Japan). After discarding the culture medium of corneal stromal cells in a 6-well plate, 500 µL TRIzol reagent was applied to each well, and the cells were scraped and transferred to a 1500-µL eppendorf (EP) tube. Each sample was added to a 1/5 volume of chloroform, mixed vigorously, and centrifuged (12,000 rpm) for 15 minutes at 4°C. Thereafter, the supernatants were absorbed, and the same volume of isopropanol was applied and centrifuged. The precipitates were added to 500 µL 75% alcohol, mixed, and centrifuged. After discarding the

Investigative Ophthalmology & Visual Science

supernatant, we dissolved RNA with diethylpyrocarbonate (DEPC) treated water and detected the concentration and purity. The extracted RNA was stored in a –80°C refrigerator for further study.

miR Microarray Analysis

TRIzol reagent (Takara Bio, Inc.) was applied to extract RNA from corneas. The 260/280-nm ratio of all RNA samples ranged from 1.9 to 2.1. By using poly(A) polymerase, the 3′ end of the miR samples was incorporated with the poly-A tail. Oligonucleotide tags were attached to the poly-A tail in later fluorescent dye staining. Samples were hybridized with microfluidic miR array chips (Agilent Technologies, Inc., Palo Alto, CA, USA) overnight. The chips were observed by an Agilent G2565BA microarray scanner, and the images were processed to generate the original signal values by Agilent Feature Extraction Software V10.10. The original signal values were normalized, logarithmically transformed, and centered using Partek Genomics Suite 6.6 (Partek, Inc., St. Louis, Missouri, USA). The data obtained were processed with Origin 2018 analysis software (OliginLab, Northampton, MA, USA).

Quantitative RT-PCR

To explore the level of miR-223-3p, specific miR stem-loop reverse transcription was performed using a miR first-strand cDNA synthesis kit (Vazyme, Nanjing, China). RT-PCR was performed by using SYBR green Master Mix (Vazyme). The primer sequences were as follows: U6, forward primer (5'-GCTTCGGCAGCACATATACTAAAAT-3') and reverse primer (5'-CGCTTCAGAATTTGCGTGTCAT-3'); miR-223-3p, forward primer (5'-TGTCAGTTTGTCAAA-3') and reverse primer (5'-CAGTGCGTGTCGTGGAGT-3'). The relative quantification of miR levels was calculated using the $2^{-\Delta\Delta Ct}$ method.

Western Blotting

The corneal stromal cells or mouse corneal tissues were harvested and lysed with RIPA reagent (Beyotime, Shanghai, China) supplemented with 1% Phenylmethylsulfonyl Fluoride (PMSF) reagent (Beyotime). Recombinant proteins (20 µg) were electrophoresed on 12.5% SDS-PAGE gels, transferred electrophoretically to PVDF membranes (Millipore, Boston, MA, USA), and blocked with 5% skimmed milk for 60 minutes. Afterward, the proteins were incubated with the corresponding primary antibodies at 4°C for 12 hours. The antibodies were as follows: anti-P62 (P0067; Sigma-Aldrich), anti-LC3B (ab192890; Abcam, Cambridge, MA, USA), anti-ATG16L1 (ab187671; Abcam), anti–TNF-α (ab183218; Abcam), anti–IL-1β (ab9722; Abcam), and anti-GAPDH (ab9485; Abcam) antibodies. On the second day, membranes were washed with TBS+Tween (TBST) thrice, incubated with the secondly antibodies horseradish peroxidase (HRP) (ab6721, Abcam) for 60 minutes, and washed again. Finally, the protein bands were visualized with ECL solution (Millipore).

Transmission Electron Microscopy

After fresh mouse corneas were harvested, the samples were quickly soaked in fixative for 3 hours and immerged in 1% osmium acid for 2 hours at 4°C. Fixed tissues were dehydrated in gradient alcohol and acetone for 15 minutes per time. Afterward, samples were infiltrated with acetone at 37°C overnight. The samples were sliced to an 80-nm thickness with an ultramicrotome. Finally, the sections were stained with 2% double uranium–lead citrate for 15 minutes and then dried for 24 hours. The specimens were examined under a transmission electron microscope (HT-7700; Hitachi Ltd., Tokyo, Japan).

Immunofluorescence

The corneas were removed from the mouse eyeball, embedded in O.C. T gel, and stored at –80°C. The specimens were sliced into 7-µm sections when used. Next, the samples were permeabilized (0.1% Triton X-100, 5 minutes), blocked (5% BSA, 30 minutes), and incubated (primary antibody, overnight) at 4°C. The antibodies were as follows: anti-P62 (P0067; Sigma-Aldrich), anti-ATG16L1 (ab187671; Abcam), and anti-GAPDH (ab9485; Abcam). After washing with PBS three times, tissue sections were incubated with Alexa Fluor–conjugated secondary antibodies (Alex488 or Alex594; Proteintech, Wuhan, China). Last, the tissue sections were visualized and images were captured with a Nikon TE2000U confocal microscope.

mRFP-GFP-LC3 Reporter Assay

AAV9-mRFP-GFP-LC3 was purchased from Hanbio Co. Ltd (Shanghai, China), and transfection was performed as per the manufacturer's protocol.[27] Briefly, mouse corneal stromal cells (1×10^5/well) were inoculated in 24-well plates. When cell fusion reached 30% to 50%, 500 µL medium and 5 µL adenovirus (10^{10}/mL, multiplicity of infection (MOI) = 500) were added. Cells were detected under a Nikon confocal laser microscope 48 hours later. The autophagic flux was investigated based on the different sensitivities of green fluorescent protein (GFP) and red fluorescent protein (RFP) to acidic environments. In an acidic environment, the GFP signal was quenched, conversely, and the RFP signal was not changed. RFP-positive puncta (red dots) indicate autolysosomes, and RFP-GFP–positive puncta (yellow dots) indicate autophagosomes.

Colony Counts

The fungal burden was assessed by enumeration of CFU. On day 5 postinfection, the corneas were harvested and homogenized in 1 mL sterile PBS. After 1:5 dilutions, 50 µL homogenates was uniformly inoculated onto Sabouroud medium plates. The plates were incubated at 28°C for 3 days. Finally, the colonies were counted and multiplied by dilution factor.

Statistical Analysis

All statistical analyses were determined by GraphPad Prism 8.0 statistical software (GraphPad Software, San Diego, CA, USA) and expressed as mean ± SD. All measurements were performed with distinct three biological replicates. The differences between the two groups were performed using unpaired two-tailed Student's *t*-tests. Comparisons between multiple groups were evaluated by one-way ANOVA followed by Tukey's post hoc test. $P < 0.05$ was considered statistically significant.

Investigative Ophthalmology & Visual Science

Results

Clinical Features and Potential Key Targets in Fungal Keratitis Mouse Models

To observe the features during the pathologic process of FK, we established a mouse model of FK. The pictures showed that the corneas of mice became opaque and swollen from the first day after fungal infection and more serious over time. On day 7, this phenomenon was resolved (Fig. 1A). From the HE staining results, obvious epithelial defects and inflammatory aggregation could be clearly observed, particularly on the fifth day after infection (Fig. 1B). We found that corneal congestion occurred in the limbus on day 1. Then corneal edema aggravated and neovascularization developed on day 3. On day 5, the tissue structure was obviously damaged and local ulcer or perforation appeared. Last, the severity of cornea infection was mitigated, and there was a trend of scar healing on day 7. The clinical score was consistent with the above results (Fig. 1C). We further analyzed our previous results of a miR chip on mouse fungal keratitis[17] and displayed differentially expressed miRs between fungal keratitis and the control by a volcano plot (adjusted $P \leq 0.05$, $|\log_2\text{Fold-change}| \geq 2$) (Fig. 1D). Among these miRs, miR-223-3p was significantly upregulated, which was further verified by PCR (Fig. 1E).

Identification and Biological Validation of ATG16L1 as miR-223-3p Target

We performed the target prediction analysis of miR-223-3p by the prediction TargetScan algorithms (http://www.targetscan.org/vert_71/) to determine the putative target for miR-223-3p. We found that autophagy-related protein 16L1 (ATG16L1) contained phylogenetically conserved miR-223-3p binding sites in the 3′UTR (Fig. 2A). Human embryonic kidney 293 cells were transfected in a dual luciferase assay reporter vector containing the ATG16L1 3′UTR sequence and cotransfected with miR-223-3p mimics or negative control (NC). Under this setting, a significant downregulation in luciferase activity was observed following transfection with a

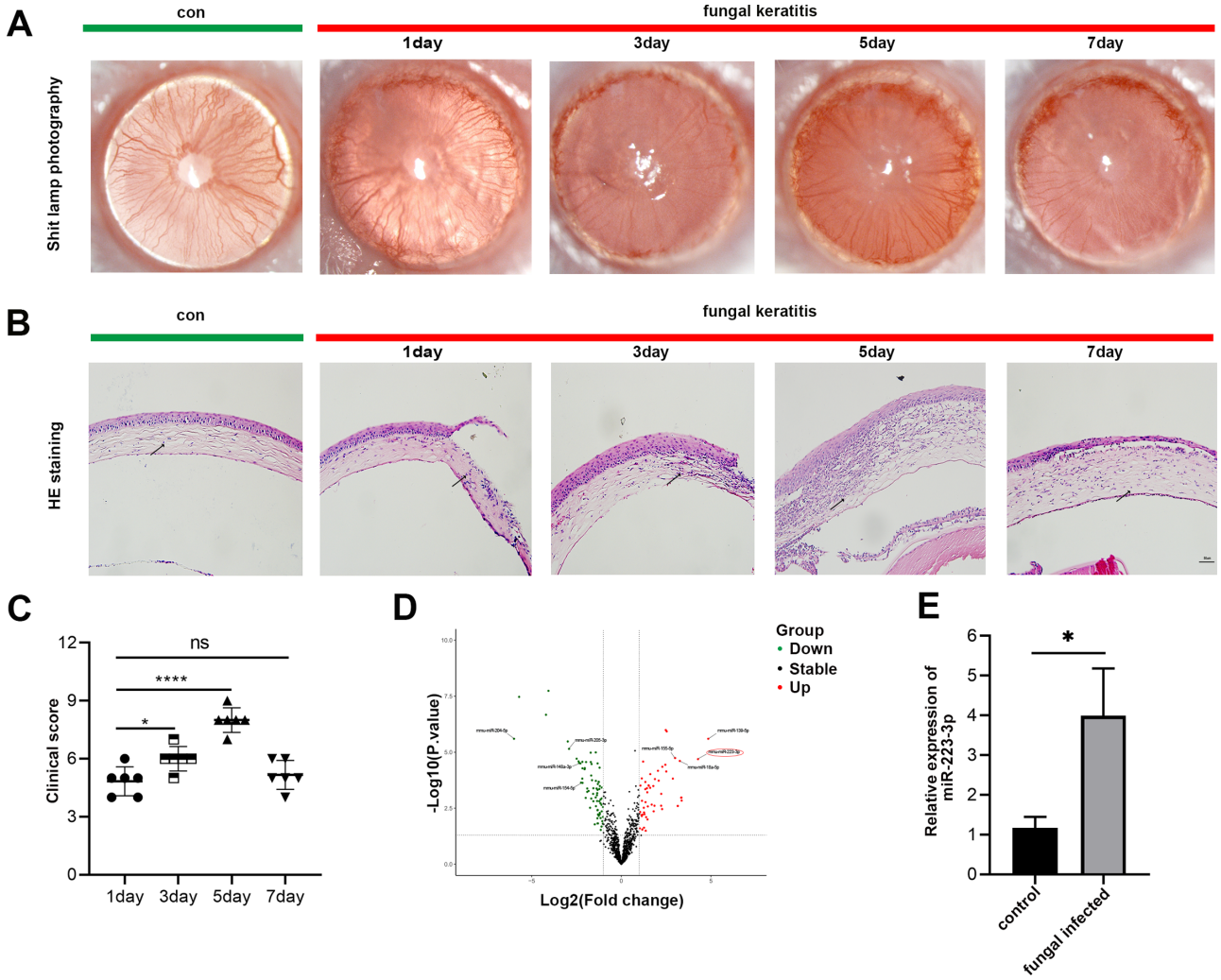

Figure 1. Clinical features and potential key targets in a mouse model of fungal keratitis. (**A**) Slit-lamp photographs of the eyes at 1, 3, 5, and 7 days after fungal infection. (**B**) Histopathologic observation of HE staining on the corneas of mice. *Scale bar*: 50 µm. The immune cells are indicated by *arrows*. (**C**) The clinical scores showed that inflammation reached its highest level at day 5. (**D**) The volcano plot displays the differentially expressed miRs between the FK and control groups. (**E**) MiR-223-3p expression was notably upregulated in the fungus-infected group. $n = 6$. *$P < 0.05$. ****$P < 0.0001$.

Investigative Ophthalmology & Visual Science

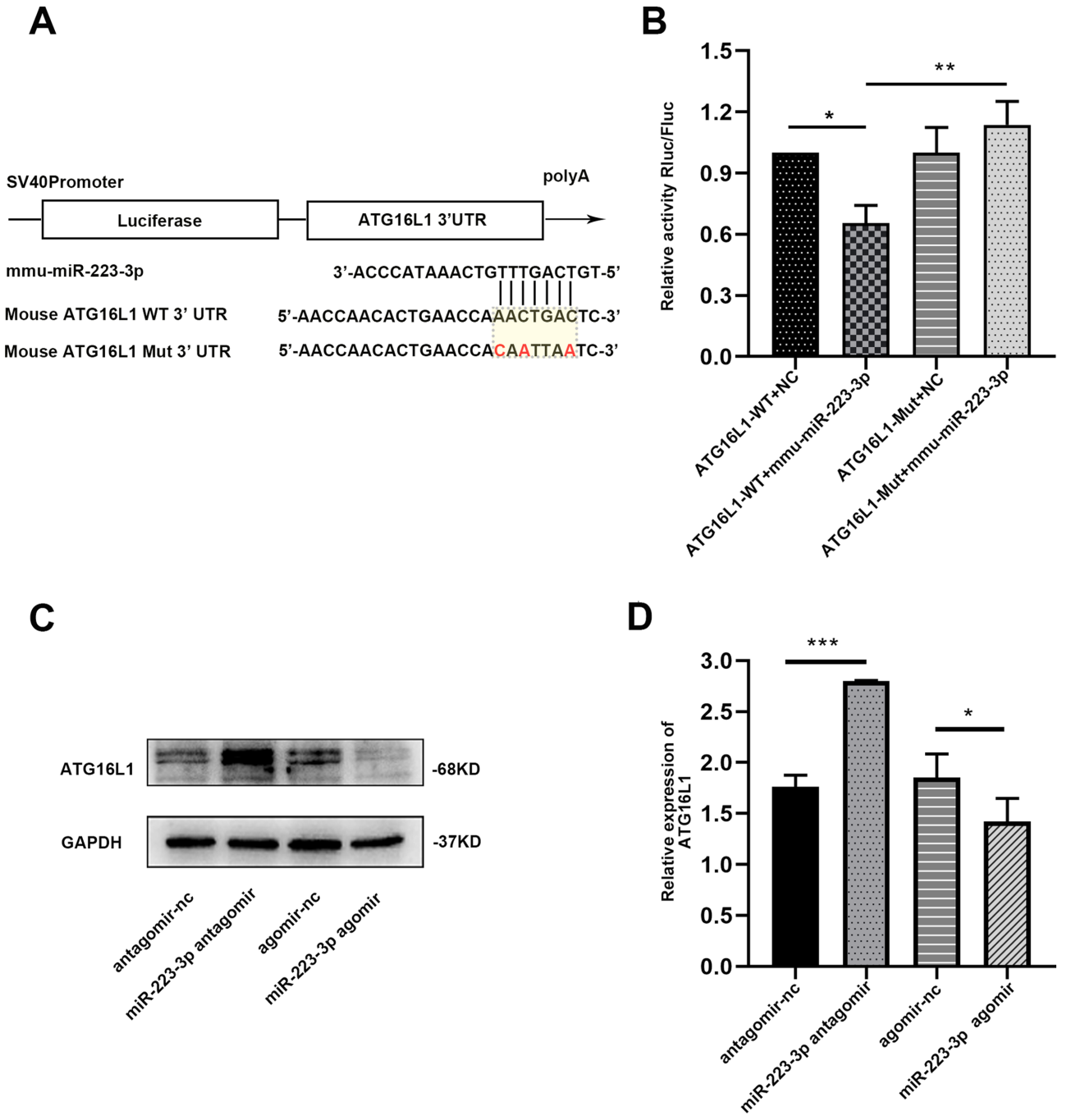

Figure 2. Identification and biological validation of ATG16L1 as a miR-223-3p target. (**A**) The binding site between miR-223-3p and the 3′UTR of ATG16L1 was predicted, and the mutation site (*red*) was constructed. (**B**) Relative luciferase activity was significantly downregulated when ATG16L1–3′UTR and miR-223-3p mimic were cotransfected. In contrast, the mutation of the complementary site of ATG16L1–3′UTR eliminated the inhibitory effect. (**C**, **D**) WB results in corneal stromal cells showed that the ATG16L1 expression was markedly upregulated in the miR-223-3p antagomir group compared with the miR-NC group. $n = 6$. $^{*}P < 0.05$. $^{***}P < 0.001$.

miR-223-3p mimic. In contrast, no significant difference in the luciferase activity was observed from the mutant construct. The results of the dual luciferase assay confirmed an interaction between 3′UTR of ATG16L1 and miR-223-3p (Fig. 2B). Western blot (WB) results in corneal stromal cells demonstrated that, compared with miR-NC treatment, the levels of ATG16L1 were upregulated in the miR-223-3p antagomir group, while the expression was downregulated in the miR-223-3p agomir group (Figs. 2C, 2D).

Autophagic Flux Was Restrained in the Cornea in a Fungal Keratitis Model

To detect autophagy activity in the process of FK, we analyzed the autophagy-associated gene expression, including P62, LC3B, and ATG16L1. WB results indicated an obvious upregulation of P62 and the LC3B II/I ratio at 5 days postinfection (Figs. 3A–C). ATG16L1 protein level was downregulated at day 5 and upregulated at day 7 postinfection

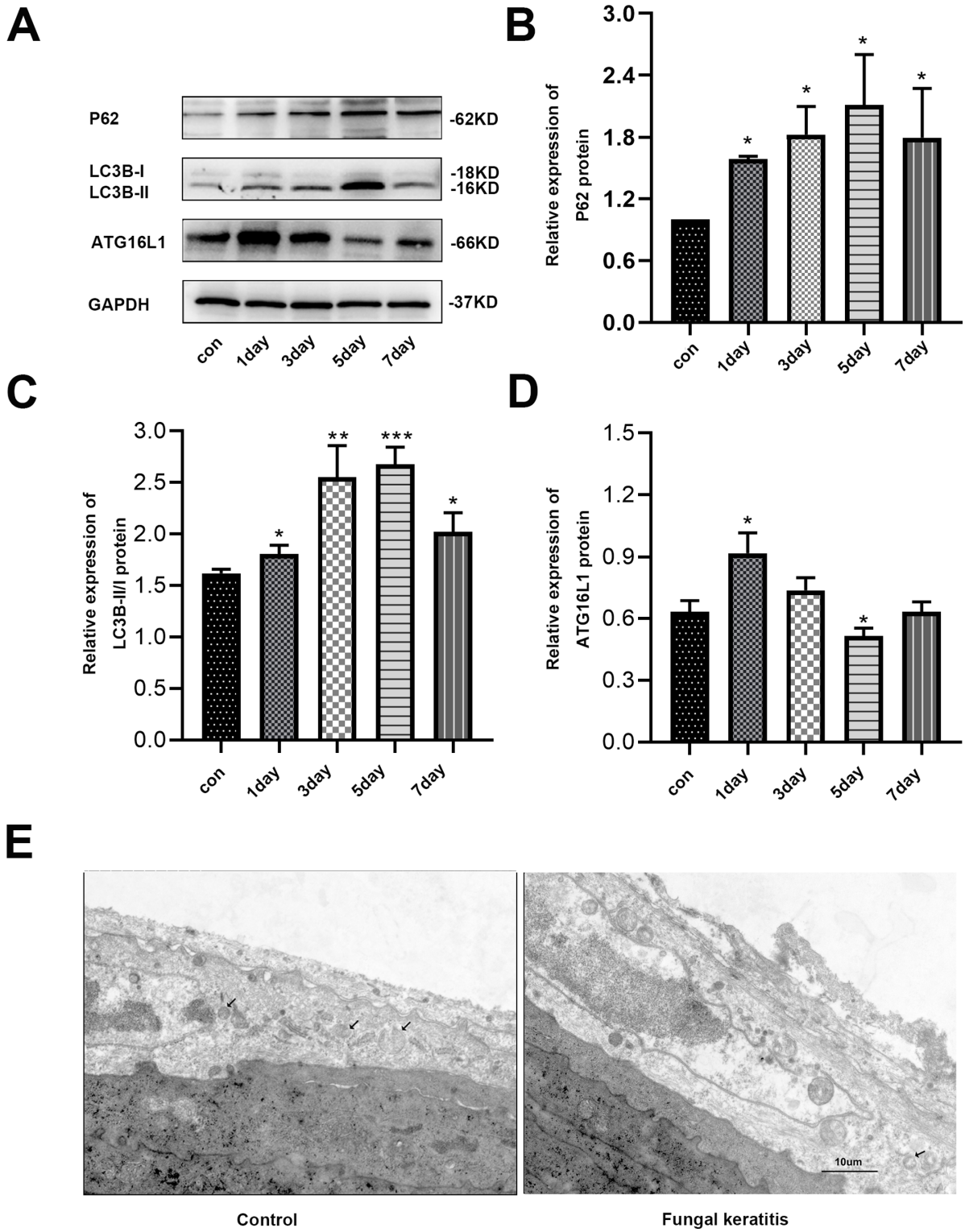

Figure 3. Autophagic flux was restrained in cornea of the FK model. (**A–D**) Western blot analysis confirmed the levels of P62, LC3B, and ATG16L1 protein in the mouse eyes 1, 3, 5, and 7 days postinfection. (**E**) Transmission electron microscopy was performed to detected autophagosomes (*black arrows*) in both groups. *Scale bar*: 10 µm. $n = 6$. *$P < 0.05$. **$P < 0.01$. ***$P < 0.001$.

(Figs. 3A, 3D). These findings indicated that the degradation of autophagy was interfered during the development of FK. We further evaluated the ultrastructure of corneal epithelium and superficial corneal stroma in FK. We found that the autophagosome in fungal-infected cornea changed with a similar morphology but in a rarer amount compared to the vehicle group (Fig. 3E), which consistently revealed that the autophagy was restrained in the FK.

Investigative Ophthalmology & Visual Science

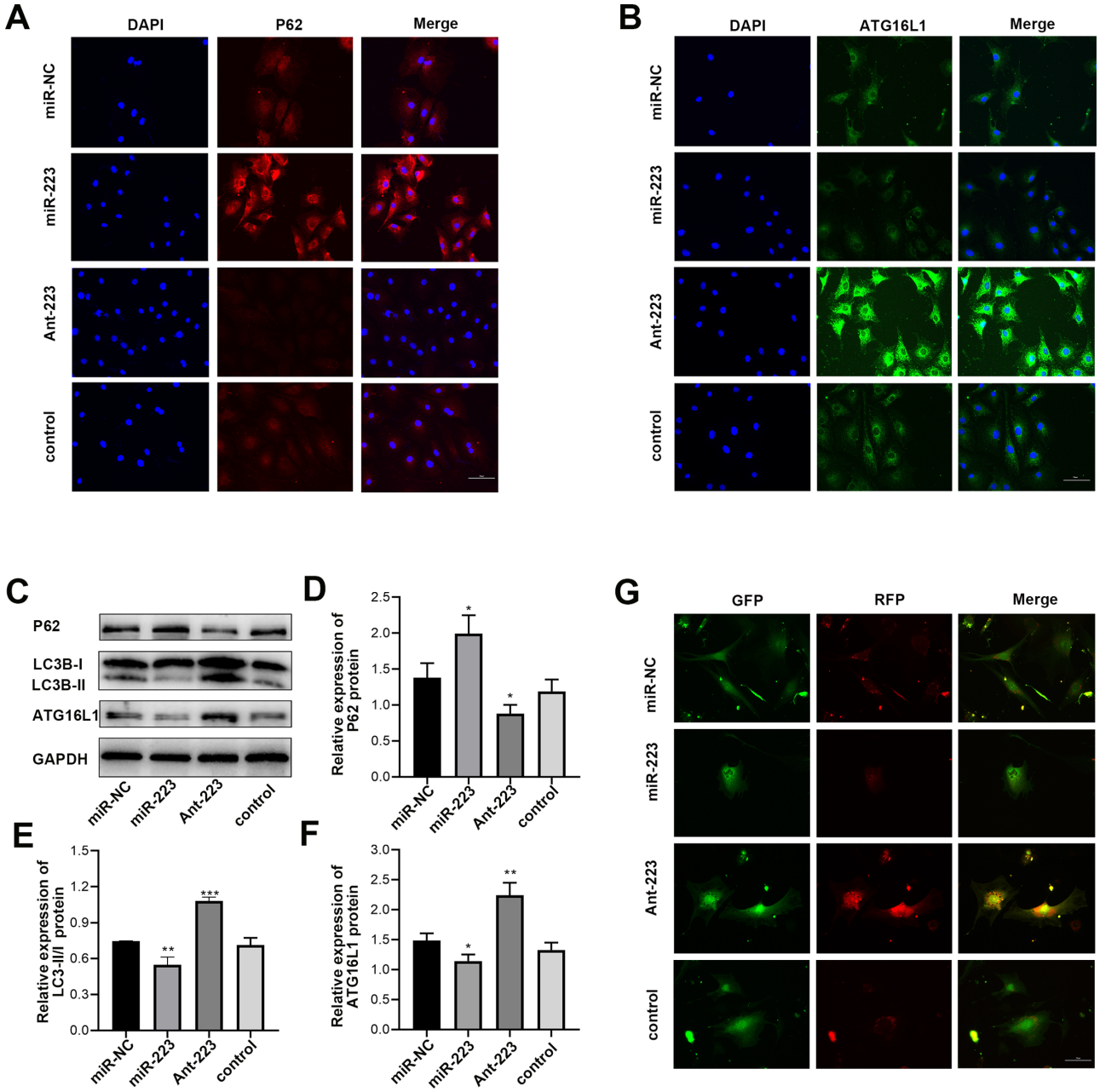

Figure 4. Suppression of miR-223-3p promoted autophagy activity in corneal stromal cells with fungi. (**A**, **B**) Immunofluorescence analysis of ATG16L1 and P62 proteins in *F. solani*–treated corneal stromal cells. (**C–F**) The expression of P62, LC3B, and ATG16L1 proteins in fungal corneal stromal cells was detected by WB. (**G**) The detection of autophagic flux in corneal stromal cells that were transfected with AAV-mRFP-GFP-LC3 for 48 hours. *Scale bar*: 70 µm. $n = 6$. *$P < 0.05$. **$P < 0.01$. ***$P < 0.001$.

Suppression of miR-223-3p Promoted Autophagy Activity in Mouse Corneal Stromal Cells Infected by Fungi

To evaluate the regulation effect of miR-223-3p on autophagy in vitro, we transfected into the mouse corneal stromal cells with respective miR agomir, antagomir, and the negative control. Immunofluorescence staining results illustrated that compared with the miR-NC group, the protein expression of P62 was upregulated in the miR-223 group and downregulated in the Ant-223 group. (Fig. 4A). Conversely, compared with miR-NC group, the levels of ATG16L1 protein were notably reduced in the miR-223 group and raised in the Ant-223 group (Fig. 4B). These conclusions were further validated in WB quantification experiments (Figs. 4C–F). To demonstrate the changes in autophagic flux, we applied the classical AAV9-mRFP-GFP-LC3 transfection method. In the miR-223 group, the autophagic flux was blocked according to the dramatically decreased amounts of red and yellow bolts. In contrast, the autophagic flux was smooth in the Ant-223 group (Fig. 4G). In conclusion, the exogenous downregulation of miR-223-3p increased the autophagy, while the upregulation of miR-223-3p suppressed the autophagy in mouse corneal stromal cells infected with fungi in vitro.

Investigative Ophthalmology & Visual Science

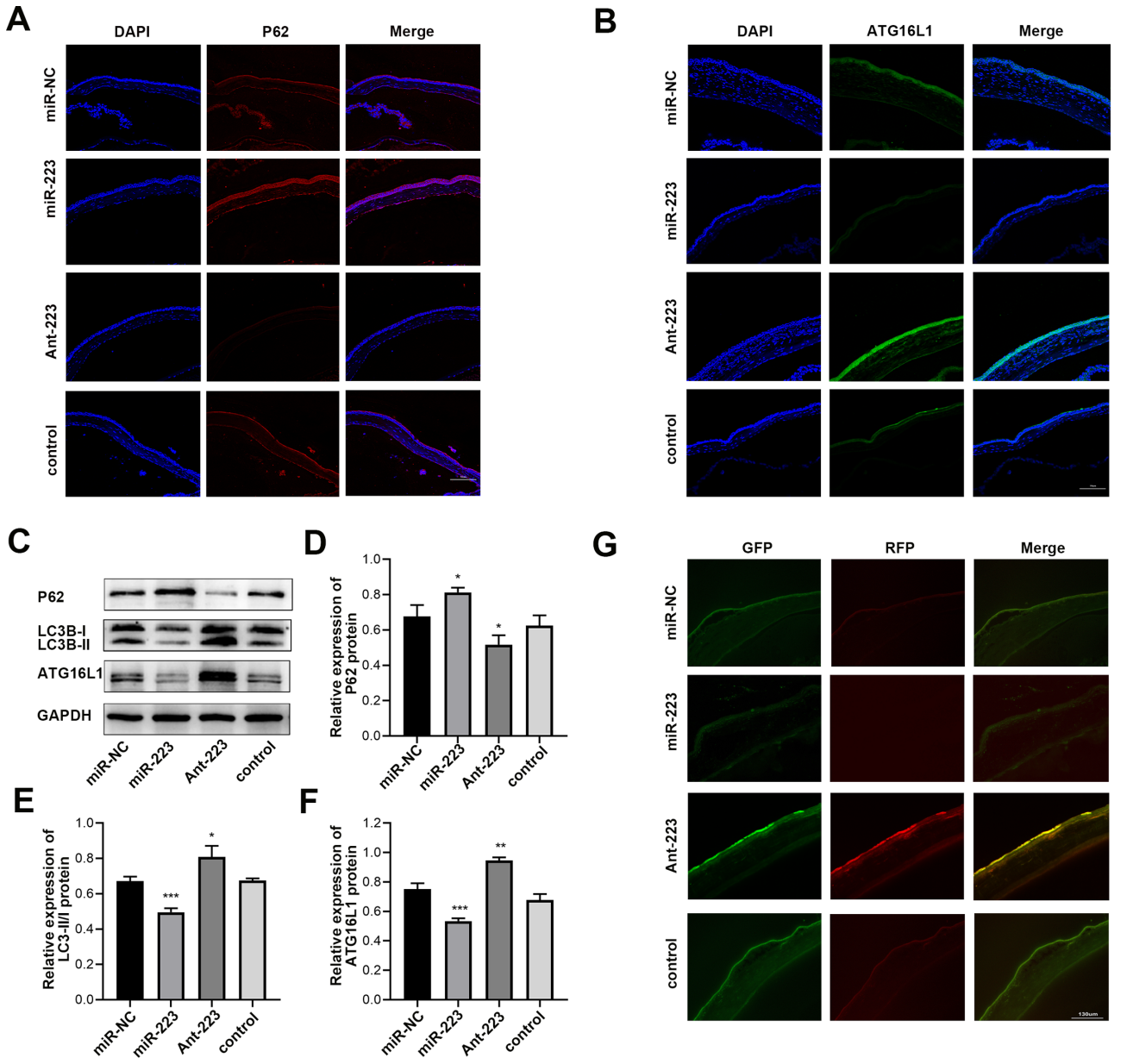

Figure 5. Inhibition of miR-223-3p increased autophagy activity in the mouse model of FK. (**A**, **B**) Immunofluorescence analysis of P62 and ATG16L1 proteins in the mouse model of FK. (**C–F**) The protein expression of P62, LC3B, and ATG16L1 in corneal tissues of model mice was tested by Western blotting. (**G**) The detection of autophagic flux in the mouse model of FK that was transfected with mRFP-GFP-LC3 adenovirus for 48 hours. *Scale bar*: 130 µm. $n = 6$. *$P < 0.05$. **$P < 0.01$. ***$P < 0.001$.

Inhibition of miR-223-3p Increased Autophagy Activity in the Mouse Model of Fungal Keratitis

We then tested the above results in a mouse animal model. The immunofluorescence staining results demonstrated that, in contrast with the miR-NC group, the level of autophagy substrate protein P62 (red) was dramatically increased in the miR-223 group, whereas the expression of P62 in Ant-223 group was observably decreased (Fig. 5A). Conversely, compared with miR-NC , ATG16L1 (green) was markedly upregulated in the Ant-223 group and dramatically downregulated in the miR-223 group (Fig. 5B). The trend of results further verified by WB quantitative experiments was consistent with the conclusions above (Figs. 5C–F). Finally, we performed the AAV9-mRFP-GFP-LC3 for autophagic flux detection. In the Ant-223 group, the conspicuous increases in red and yellow fluorescence represented free autophagy flux, whereas in the miR-223 group, the prominent decreases in the amounts of red and yellow fluorescence suggested a block in the flow of the autophagy pathway (Fig. 5G). In summary, exogenous upregulation of miR-223-3p restrained the autophagy of FK, and the inhibition of miR-223-3p facilitated the autophagy activity of FK in vivo.

Downregulation of miR-223-3p Reduced Inflammation and Improved Clinical Scores of Fungal Keratitis

On day 5 postinfection, slit-lamp photography was performed. The results showed that in comparison with miR-NC, corneal edema and turbidity in the miR-223 group were

Investigative Ophthalmology & Visual Science

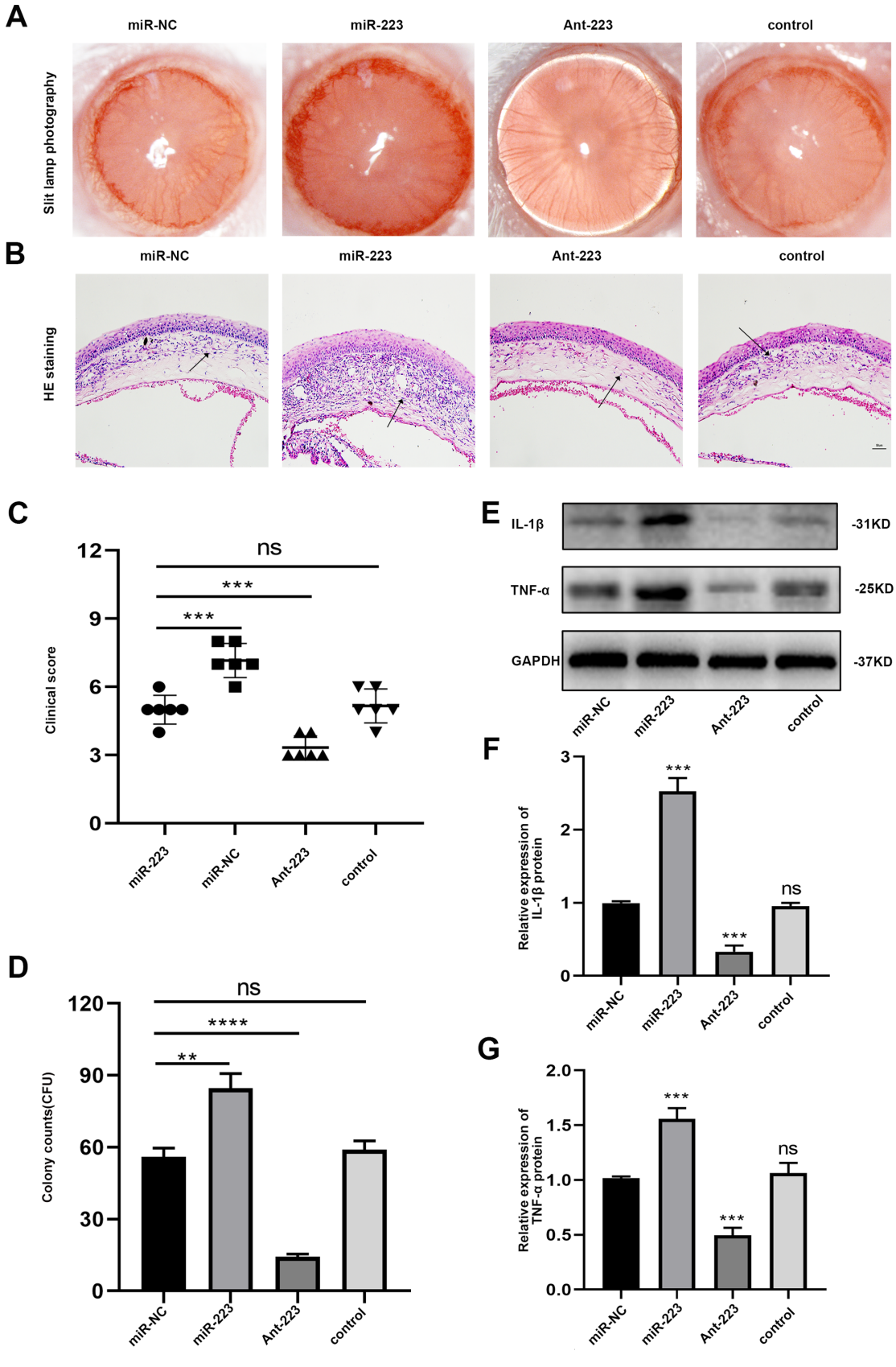

Figure 6. Downregulation of miR-223-3p reduced inflammation and improved clinical scores of FK. (**A**) Slit-lamp biomicroscope photographs of the mouse eyes at 5 days postinfection. (**B**) Histopathologic observation of HE staining on the corneas of mice. *Scale bar*: 50 µm. The immune cells are indicated by *arrows*. (**C**) The clinical scores showed that the inflammation of the Ant-223 group was notably decreased compared with that of the miR-NC group. (**D**) The fungal colonies in the corneas of mice in each group. (**E–G**) The protein levels of IL-1β and TNF-α in the miR-223 group were notably increased in contrast with that in the miR-NC group. $n = 6$. $^{**}P < 0.01$. $^{***}P < 0.001$. $^{****}P < 0.0001$.

Investigative Ophthalmology & Visual Science

more serious, and abundant neovascularization grew in the corneal limbus. However, corneal edema and turbidity in the Ant-223 group were alleviated, and rare neovascularization was observed (Fig. 6A). Compared with the control group, corneal edema and neutrophil infiltration were alleviated in the Ant-223 group, while the pathologic damage in the miR-223 group was severe, manifested as corneal edema, the irregular arrangement of epithelial structure, and the aggravation of neutrophil infiltration (Fig. 6B). The clinical scores illustrated that, in contrast with the miR-NC group, the Ant-223 group was lower, while the miR-223 group was higher (Fig. 6C).

After treatment with miR-223-3p inhibitor, the colonies in the mouse corneas were significantly reduced (Fig. 6D). Therefore, we speculate that the downregulation of miR-223-3p can accelerate recovery and improve the clinical symptoms of FK. Then, we conducted a quantitative WB experiment to detect the inflammatory-related indicators IL-1β and TNF-α. The results illustrated that in comparison with the miR-NC group, the protein levels of IL-1β and TNF-α in the miR-223 group were notably increased, in contrast to the Ant-223 group, which were decreased (Figs. 6E–G). In summary, we concluded that the exogenous increased miR-223-3p aggravated the inflammatory response of FK; conversely, the downregulation of miR-223-3p improved clinical manifestations and reduced the inflammatory response.

Discussion

Fungal keratitis is a severe infectious disease that might lead to irreversible visual impairment and eyeball loss.[28,29] To date, plant-associated *Fusarium* infection is the most common cause of FK in northern China.[30] However, due to its strong virulence and fungal invasiveness, there are no effective antifungal agents.[31,32] Excessive inflammation caused by increased corneal inflammatory cell infiltration is an important factor in corneal injury in FK,[5] so it is very important to regulate the progression of corneal inflammation. Increasingly, studies have explored that miR-223-3p, as a crucial cell modulator, is involved in mediating infection and inflammation.[14] In particular, a previous study detected the miR expression profile in the cornea of patients infected with fungi and suggested the elevated expression of miR-223-3p.[18] Consistent with this, we also validated an increase of miR-223-3p level in a mouse model infected with *F. solani*.[17] At present, the precise function of miR-223-3p in FK is still vague.

To determine the precise functions of miR-223-3p, which is significantly upregulated in FK, we employed bioinformatics screening to predict the downstream target of miR-223-3p. We found that the 3′UTR of autophagy-related protein 16-1 (ATG16L1) has a putative junction for miR-223-3p. We performed dual luciferase reporter analysis and found that miR-223-3p dramatically decreased the luciferase levels of the ATG16L1 3′ UTR. Furthermore, the negative regulatory influence of miR-223-3p on the downstream gene ATG16L1 were also determined by WB. ATG16L1 plays an essential role in autophagy and can bind to ATG5–ATG12 to form a conjugate complex, activate downstream molecules, and promote the conversion of LC3-I to LC3-II.[33,34] Li et al.[35] confirmed that miR-223-3p inhibits autophagy and aggravates inflammation of the central nervous system by targeting ATG16L1. We thus speculate that miR-223-3p may act as an essential autophagy-associated miR that is involved in the occurrence and progression by affecting the autophagy pathway in FK.

Autophagy is an evolutionarily conserved process in eukaryotes that degrades longevity proteins and damaged organelles through lysosomes and regulates intracellular homeostasis.[19] Accumulating evidence supports that inflammation is an essential regulator of autophagy.[36,37] Briefly, autophagy modulates inflammation by influencing the secretion of inflammatory cytokines and altering the inflammatory cell survival environment.[38] Recent studies have illustrated that autophagy also plays a key role in the pathologic progress of FK.[39] Autophagy can reduce the severity of *A. fumigatus* keratitis by regulating the recruitment of neutrophils and balancing the production of proinflammatory and anti-inflammatory cytokines.[21] Likewise, our study also found that autophagic flux was restrained in the cornea of a FK model. Further experiments need to be done to determine the regulation of miR-223-3p on autophagy in FK. We revealed that the inhibition of miR-223-3p increased the LC3B II/I ratio and ATG16L1 protein levels, whereas the expression of P62 was reduced. However, following miR-223-3p overexpression, the opposite results were obtained. Considering that autophagy is a dynamic process, we employed a mRFP-GFP-LC3 reporter assay to detect autophagic flux. The data demonstrated that reducing miR-223-3p enhanced the activity of autophagic flux. In summary, our research identified that downregulating miR-223-3p can improve ATG16L1-activated autophagy in FK.

It was mentioned earlier that miR-223-3p is involved in several inflammatory diseases.[14] We next explored whether miR-223-3p played roles in *F. solani*–triggered corneal inflammation. Our study revealed that the inflammatory response and clinical scores were alleviated by inhibiting the expression of miR-223-3p. Prior studies illustrated that IL-1β and TNF-α are closely related to the defense against congenital antimicrobial infection and are widely involved in the induction and release of a variety of inflammatory factors.[40–42] As expected, the expression of inflammatory proteins was reduced by suppressing miR-223-3p expression. In addition, reducing miR-223-3p significantly decreased the fungal colonies in mouse corneas. Consistent with this, the silencing of miR-223-3p expression could attenuate the damage in experimental arthritis. We therefore hypothesized that miR-223-3p might have proinflammatory effects in multiple diseases and alter the inflammatory response of FK via regulating the expression of miR-223-3p.

In conclusion, our data demonstrated for the first time that miR-223-3p was overexpressed in FK and that inhibiting miR-223-3p could promote autophagy and alleviate inflammation by targeting ATG16L1. We believe that new interventions to treat FK by silencing miR-223-3p will be feasible in the future.

Acknowledgments

Supported by the National Natural Science Foundation of China, Beijing, China (grant 81870636).

Disclosure: **H. Tang**, None; **Y. Lin**, None; **L. Huang**, None; **J. Hu**, None

References

1. Guest JM, Singh PK, Revankar SG, Chandrasekar PH, Kumar A. Isavuconazole for treatment of experimental fungal endophthalmitis caused by *Aspergillus fumigatus*. *Antimicrob Agents Chemother*. 2018;62(11):e01537–18.
2. Bongomin F, Gago S, Oladele RO, Denning DW. Global and multi-national prevalence of fungal diseases-estimate precision. *J Fungi (Basel)*. 2017;3(4):57.
3. Todokoro D, Suzuki T, Tamura T, et al. Efficacy of luliconazole against broad-range filamentous fungi including *Fusarium solani* species complex causing fungal keratitis. *Cornea*. 2019;38(2):238–242.
4. Pearlman E, Sun Y, Roy S, et al. Host defense at the ocular surface. *Int Rev Immunol*. 2013;32(1):4–18.
5. He D, Hao J, Zhang B, et al. Pathogenic spectrum of fungal keratitis and specific identification of *Fusarium solani*. *Invest Ophthalmol Vis Sci*. 2011;52(5):2804–2808.
6. Vaitkienė S, Daugelavičius R, Sychrová H, Kodedová M. Styrylpyridinium derivatives as new potent antifungal drugs and fluorescence probes. *Front Microbiol*. 2020;11:2077.
7. Cao M, Wu Z, Lou Q, et al. Dectin-1-induced RIPK1 and RIPK3 activation protects host against *Candida albicans* infection. *Cell Death Differ*. 2019;26(12):2622–2636.
8. Hsin J-P, Lu Y, Loeb GB, Leslie CS, Rudensky AY. The effect of cellular context on miR-155-mediated gene regulation in four major immune cell types. *Nat Immunol*. 2018;19(10):1137–1145.
9. Sales G, Coppe A, Bicciato S, Bortoluzzi S, Romualdi C. Impact of probe annotation on the integration of miR-mRNA expression profiles for miR target detection. *Nucleic Acids Res*. 2010;38(7):e97.
10. Yeruva L, Pouncey DL, Eledge MR, et al. MicroRNAs modulate pathogenesis resulting from chlamydial infection in mice. *Infect Immun*. 2017;85(1):e00768–e00816.
11. Haneklaus M, Gerlic M, O'Neill LAJ, Masters SL. miR-223: infection, inflammation and cancer. *J Intern Med*. 2013;274(3):215–226.
12. Li X, He S, Li R, et al. *Pseudomonas aeruginosa* infection augments inflammation through miR-301b repression of c-Myb-mediated immune activation and infiltration. *Nat Microbiol*. 2016;1(10):16132.
13. Wang X, Chi J, Dong B, et al. MiR-223-3p and miR-22-3p inhibit monosodium urate-induced gouty inflammation by targeting NLRP3. *Int J Rheum Dis*. 2021;24(4):599–607.
14. Tian J, Zhou D, Xiang L, et al. MiR-223-3p inhibits inflammation and pyroptosis in monosodium urate-induced rats and fibroblast-like synoviocytes by targeting NLRP3. *Clin Exp Immunol*. 2021;204(3):396–410.
15. Wang X, Ding YY, Chen Y, et al. MiR-223-3p alleviates vascular endothelial injury by targeting IL6ST in Kawasaki disease. *Front Pediatr*. 2019;7:288.
16. Long F-Q, Kou C-X, Li K, Wu J, Wang Q-Q. MiR-223-3p inhibits rTp17-induced inflammasome activation and pyroptosis by targeting NLRP3. *J Cell Mol Med*. 2020;24(24):14405–14414.
17. Guo Q, Lin Y, Hu J. Inhibition of miR-665-3p enhances autophagy and alleviates inflammation in *Fusarium solani*-induced keratitis. *Invest Ophthalmol Vis Sci*. 2021;62(1):24.
18. Boomiraj H, Mohankumar V, Lalitha P, Devarajan B. Human corneal microRNA expression profile in fungal keratitis. *Invest Ophthalmol Vis Sci*. 2015;56(13):7939–7946.
19. Fukuda T, Kanki T. Atg43, a novel autophagy-related protein, serves as a mitophagy receptor to bridge mitochondria with phagophores in fission yeast. *Autophagy*. 2021;17(3):826–827.
20. Xie Y-P, Lai S, Lin Q-Y, et al. CDC20 regulates cardiac hypertrophy via targeting LC3-dependent autophagy. *Theranostics*. 2018;8(21):5995–6007.
21. Li C, Li C, Lin J, et al. The role of autophagy in the innate immune response to fungal keratitis caused by *Aspergillus fumigatus* infection. *Invest Ophthalmol Vis Sci*. 2020;61(2):25.
22. Hu J, Wang X, Cui X, Kuang W, Li D, Wang J. Quercetin prevents isoprenaline-induced myocardial fibrosis by promoting autophagy via regulating miR-223-3p/FOXO3. *Cell Cycle*. 2021;20(13):1253–1269.
23. Zou J, Dong X, Wang K, Shi J, Sun N. Electroacupuncture inhibits autophagy of neuron cells in postherpetic neuralgia by increasing the expression of miR-223-3p. *Biomed Res Int*. 2021;2021:6637693.
24. Wang H, Chen J, Zhang S, et al. MiR-223 regulates autophagy associated with cisplatin resistance by targeting FBXW7 in human non-small cell lung cancer. *Cancer Cell Int*. 2020;20:258.
25. Hu J, Hu Y, Chen S, et al. Role of activated macrophages in experimental *Fusarium solani* keratitis. *Exp Eye Res*. 2014;129:57–65.
26. Wu TG, Wilhelmus KR, Mitchell BM. Experimental keratomycosis in a mouse model. *Invest Ophthalmol Vis Sci*. 2003;44(1):210–216.
27. Hale CM, Cheng Q, Ortuno D, et al. Identification of modulators of autophagic flux in an image-based high content siRNA screen. *Autophagy*. 2016;12(4):713–726.
28. Dai S, Dulcey AE, Hu X, et al. Methyl-β-cyclodextrin restores impaired autophagy flux in Niemann-Pick C1-deficient cells through activation of AMPK. *Autophagy*. 2017;13(8):1435–1451.
29. Brown L, Leck AK, Gichangi M, Burton MJ, Denning DW. The global incidence and diagnosis of fungal keratitis. *Lancet Infect Dis*. 2021;21(3):e49–e57.
30. Xie L, Zhong W, Shi W, Sun S. Spectrum of fungal keratitis in North China. *Ophthalmology*. 2006;113(11):1943–1948.
31. Kuo M-T, Chen J-L, Hsu S-L, Chen A, You H-L. An omics approach to diagnosing or investigating fungal keratitis. *Int J Mol Sci*. 2019;20(15):3631.
32. Ortega-Rosales A, Quizhpe-Ocampo Y, Montalvo-Flores M, Burneo-Rosales C, Romero-Ulloa G. A case of fungal keratitis due to *Fusarium solani* after an indigenous healing practice. *IDCases*. 2019;18:e00618.
33. Ji C, Zhao H, Li D, et al. Role of Wdr45b in maintaining neural autophagy and cognitive function. *Autophagy*. 2020;16(4):615–625.
34. Feng C-W, Chen N-F, Sung C-S, et al. Therapeutic effect of modulating TREM-1 via anti-inflammation and autophagy in Parkinson's disease. *Front Neurosci*. 2019;13:769.
35. Li Y, Zhou D, Ren Y, et al. Mir223 restrains autophagy and promotes CNS inflammation by targeting ATG16L1. *Autophagy*. 2019;15(3):478–492.
36. Jang YJ, Kim JH, Byun S. Modulation of autophagy for controlling immunity. *Cells*. 2019;8(2):138.
37. Larabi A, Barnich N, Nguyen HTT. New insights into the interplay between autophagy, gut microbiota and inflammatory responses in IBD. *Autophagy*. 2020;16(1):38–51.
38. Liu Z, Chen D, Chen X, et al. Autophagy activation protects ocular surface from inflammation in a dry eye model in vitro. *Int J Mol Sci*. 2020;21(23):8966.
39. Lin J, Lin Y, Huang Y, Hu J. Inhibiting miR-129-5p alleviates inflammation and modulates autophagy by targeting ATG14 in fungal keratitis. *Exp Eye Res*. 2021;211:108731.

40. Aarreberg LD, Esser-Nobis K, Driscoll C, Shuvarikov A, Roby JA, Gale M. Interleukin-1β induces mtDNA release to activate innate immune signaling via cGAS-STING. *Mol Cell*. 2019;74(4):801–815.e6.
41. Karki R, Sharma BR, Tuladhar S, et al. Synergism of TNF-α and IFN-γ triggers inflammatory cell death, tissue damage, and mortality in SARS-CoV-2 infection and cytokine shock syndromes. *Cell*. 2021;184(1):149–168.e17.
42. Drummond RA, Swamydas M, Oikonomou V, et al. CARD9+ microglia promote antifungal immunity via IL-1β- and CXCL1-mediated neutrophil recruitment. *Nat Immunol*. 2019;20(5):559–570.

Investigative Ophthalmology & Visual Science